Near-infrared emitting quantum dots: Recent progress on their synthesis and characterization

Jothirmayanantham Pichaandi and Frank C.J.M. van Veggel

March 2014

Near-Infrared Emitting Quantum Dots: Recent Progress on Their Synthesis and Characterization

Jothirmayanantham Pichaandi and Frank C. J. M. van Veggel*

Department of Chemistry, University of Victoria, P.O. Box 3065, Victoria, British Columbia, Canada, V8W 3V6

* corresponding author email: fvv@uvic.ca

Contents

Abstract

Near-infrared emitting lead-based quantum dots (QD) have gained considerable attention in the last decade due to their potential applications in for instance solar cells, bioimaging, telecommunications, and quantum computing. These QDs can be tuned to emit from 750 to 3700 nm which makes them very viable for the aforementioned applications. Although the synthesis was developed over the last decade, which had led to fairly uniform and narrow size distribution of lead-based quantum dots, the stability of these QDs under atmospheric conditions has rather been a big challenge. The stability of these QDs is of course of paramount importance for various applications. A passivation shell is normally grown over the quantum dots to form a core/shell structure which in turn improves the stability. There are semiconductors which potentially could grow over PbSe or PbS QDs by the conventional epitaxial method, such as EuS, CdS, and CdSe. However, the conventional epitaxial method of growing a larger band gap as the passivating shell has not yet yielded the desired core/shell structure for PbSe or PbS QDs. Furthermore, a few groups have worked on improving the stability of the lead-based QDs. The first part of the review focuses on the synthesis of the lead-based QDs and what modifications have been applied to improve the quality of the nanocrystals. The second part of the review will emphasize the core/shell synthesis of PbSe/CdSe and PbS/CdS and how their structure has been validated. The third part of the review will focus on the surface modification of these QDs with different methods and what challenges still lie ahead. The fourth part will discuss the optical properties of the core and core/shell QDs. The last part of the review will briefly deal with NIR QDs other than lead-based ones. Finally, we will conclude what challenges lie ahead in the field of lead-based QDs and their application in the field of biology.

Keywords: Infrared Emission, quantum dots, lead-based quantum dots, cation exchange, surface modification, photostability, core-shell quantum dots.

1. Introduction

The name quantum dot was coined by Mark Reed at Yale University in 1982 because of their size-dependent optical properties due to the bang gap change in the nano-size regime. The band gap changes with discrete energy levels observed at the nano-size regime [1]. The standard text book example for this is to solve Schrödinger's wave equation for a particle, with only kinetic and potential energy, in a box. The spacing of the discrete energy levels increases if the box dimensions decrease. Quantum confinement is observed as long as the size of the material is smaller than the Bohr exciton radius, which is the characteristic length scale for this phenomenon. Due to this, the band gap changes as the size of the quantum dot changes. For instance, cadmium selenide (CdSe) has a Bohr exciton radius of around 6 nm while lead selenide (PbSe) has a Bohr exciton radius of 46 nm. This means that to exert quantum size effects on CdSe the size "of the box" must be smaller than 6 nm, whereas for PbSe the size of the box only has to be smaller than 46 nm [2]. The size-dependent optical properties of quantum dots have made them potentially a big candidate in a large number of applications ranging from solar cells, telecommunications, quantum computing, to nanomedicine [3]. Over the last 2 decades, there has been considerable effort to improve the properties of quantum dots especially their stability in various conditions and luminescence efficiency. For instance, cadmium-based quantum dots (CdSe, CdS, CdTe, CdSeS are II-VI semiconductors) have been synthesized with very high photoluminescence quantum yield and have been used for a variety of applications mentioned above [4]. These cadmium-based quantum dots emit in the visible region of the light spectrum, because their band gap can be tuned between 3.5 to 1.7 eV [5], whereas there are quantum dots like InAs and InP (III-V semiconductor), PbSe and PbS (IV-VI semiconductor), HgTe (II-VI semiconductor), Ag_2S and Ag_2Se (I-VI semiconductor), $CuInS_2$, and $CuInSe_2$ ((I-III-VI_2 semiconductors) which emit in the near- infrared (750 to 5000 nm) [6-7]. These values

are all based on room temperature photoluminescence (PL) measurements. The PL of the QDs exhibit a red shift when measured at lower temperatures, hence the emission for the biggest mercury based QD can be beyond 5000 nm as well. This review will mainly focus on the synthesis and characterization of near-infrared light emitting quantum dots, especially the lead-based ones. Visible light emitting quantum dots have been researched a lot and considerable improvements have been achieved in the synthesis yield, luminescence, and stability [8]. The near-infrared QDs have a big advantage over the visible QDs in certain applications like telecommunications, solar cells, and bio- imaging. Of all the infrared quantum dots, lead-based QDs have the highest luminescence efficiency of 60 to 70% [6, 9]. Their size can easily be tuned to the make them emit in the required wavelength starting from 750 nm to 3700 nm [9-10]. Some of the advantages of near infra-red QDs, including the lead- based quantum dots, are elucidated below:

1. Emission in the near infra-red. So these QDs potentially absorb visible and near-infrared photons as well. This could potentially improve the efficiency of the solar cells.
2. Emission can be tuned perfectly for the telecommunications wavelength (C-band at 1550 nm).
3. Emission and excitation of these QDs could be tuned to lie within the biological window. The biological window (700 to 1100) is the region where tissues do not scatter the light as much as in the UV-visible, there is less absorption, and there is almost no autofluorescence. Employing these QDs for bio-imaging could potentially help in imaging deeper than the current imaging agents like fluorescent proteins, dyes, and visible emitting QDs.
4. Potential application in near-infrared LEDs.
5. High quantum yield (>70%) typically for smaller quantum dots (1.5 to 4 nm) and about 20

to 30 % for larger sized quantum dots (5 to 10 nm).

However, there are some inherent disadvantages to these lead-based quantum dots as well:

1. Poor stability in ambient atmosphere leading to oxidation resulting in the loss of emission.
2. Poor colloidal stability in (buffered) aqueous environment (which is especially important for biological applications) after surface modification. The process of surface modification on lead-based QDs is inherently difficult when compared to that of the cadmium-based QDs.
3. Processing of the colloidal QDs with polymers (in-situ polymerization of the monomer along with the colloidal QDs at temperatures above 40 ^{o}C) for various applications is very hard due to aggregation and loss of luminescence after their surface modification.

There has been considerable development in the field of the synthesis and stability of the lead-based QDs which will be detailed in this review. The characterization of the QDs will also be elucidated in some detail. Following that, the review will focus on surface modification of QDs for applications in biology. Modifications for other applications will briefly be mentioned as well. The third part will deal with the luminescence spectroscopy of these QDs under various conditions. NIR QDs other than lead-based ones will be described briefly in the last part of the review. Finally, we will conclude on how the field has progressed over the years and the challenges that we see to advance the field.

2. Synthesis of Lead-based QDs

2.1 Synthesis of PbSe QDs

The synthesis of the lead-based quantum dots is normally done through the typical hot injection method, with a lead precursor at a high temperature while a sulphur or selenium source is rapidly injected, resulting in the formation of the quantum dots [11-12]. The most common solvent is

octadecene with oleic acid as the ligand (i.e. stabilizer) of the QDs [5, 13]. The lead oleates are formed by reacting a lead salt, e.g. $PbCl_2$, PbO, $Pb(CH_3COO)_2$, with oleic acid as the coordinating ligand and octadecene as the non-coordinating solvent. In some cases diphenyl ether is used as the non-coordinating solvent [14-15]. The synthesis was developed by several groups to obtain highly crystalline and photoluminescent QDs. The first liquid phase (colloidal) synthesis of PbSe QDs was reported by Murray and coworkers [5] followed by similar work from Giyot-Sinonnest *et al.* [16] and Krauss *et al.* [17]. Following this, Colvin and coworkers reported a synthetic methodology to prepare monodisperse PbSe QDs in presence of a non-coordinating solvent [18]. The presence of non-coordinating solvent enabled them to synthesize monodisperse quantum dots with sizes ranging 3 to 10 nm. The monodisperse QDs also exhibited high photoluminescence (PL) quantum yield of about 85 % which was measured using IR-25 dye as the standard. The stability of PbSe QDs synthesized with the developed procedures was studied by our group which suggests that when exposed to light, the oxidation of the QDs were accelerated and a white precipitate was observed at the bottom of the solution [19]. The formation of this white precipitate implies the formation of lead oxide and the ligands being removed from the surface, resulting in precipitation. Furthermore, in presence of a xenon lamp irradiation and under oxygen atmosphere the oxidation is even more rapid (Figure 1). This is observed both in solution as well as in the solid state. Figure 1 and 2 below show the emission shift towards the blue and the quenching of the emission under these conditions. In Figure 1, we observe a blue shift due to very long exposure to oxygen and light, whereas in Figure 2 the PL gets quenched which suggests that the QDs do not oxidize rapidly on exposure to oxygen. A similar stability study was explored with lifetimes, optical measurements, and XPS (X-ray Photo-electron Spectroscopy) on PbSe QDs in presence and absence of oxygen [20-21]. Generally, a semiconductor material with a large bandgap is grown over the core QDs to passify the surface so that the dangling bonds are

minimized. These are generally called type I core/shells as the hole and the electron are confined in the core and the shell does not contribute much to the wavefunctions. The second option is to grow a shell with a smaller band gap in which case the hole and electron are (mostly) confined in the shell. Depending on the thickness of the shell emission wavelength can be tuned. The third option is to grow material where the valence band and the conduction band edges are either lower or higher than the respective level in the core QDs. This is called type II core/shell as the electron hole pair will not be confined to the core QDs. Depending on the relative position of the top of the valence band or the bottom of the conduction band for the core/shell QDs, the hole and electron will spatially be separated. This aids in tuning the emission wavelength of the core/shell QDs to a large extent by choosing the right semiconductor shell material and the thickness of the shell [22]. In order to enhance the stability of the PbSe QDs, a shell of PbS was grown over PbSe. Interestingly, no remarkable difference in stability was observed between the core and core/shell QDs. After the growth of the shell, the QDs show a red shift of the PL which could either be due to the diffusion of shell material into the core forming an alloyed heterostructured material or the core nanocrystals which could have grown bigger during the shell growth. The shell growth might not have happened and it could have resulted in a completely alloyed $PbSe_xS_{(1-x)}$ structure resulting in a red shift. The presence of extra lead and sulphur could have made the QDs bigger than the core after the supposed shell reaction resulting in the red shift. However, there are reports that suggest that these are type II core/shell structures where the electron is in the conduction band of the core while the hole is in the shell [11, 14-15]. This will result in an overall red shift in the emission when compared to just the core QDs. This theory of PbSe/PbS being a type II core/shell structure has, in our view, not yet been proved convincingly. We are of the opinion that these are heterostructured nanomaterials (size of the core/shell larger than the core) rather than proper core/shell nanomaterials. Our point of view comes from the fact

that the optical properties and the TEM do not show any convincing data to support a core/shell structure. It is very hard to get concrete evidence for a core/shell structure from the TEM images as there was no contrast difference. The optical properties observed after the supposed core/shell growth also do not provide proof for a core/shell. One possible solution to this is to perform energy- dependent XPS at a synchrotron source which will reveal the structure of the QDs.

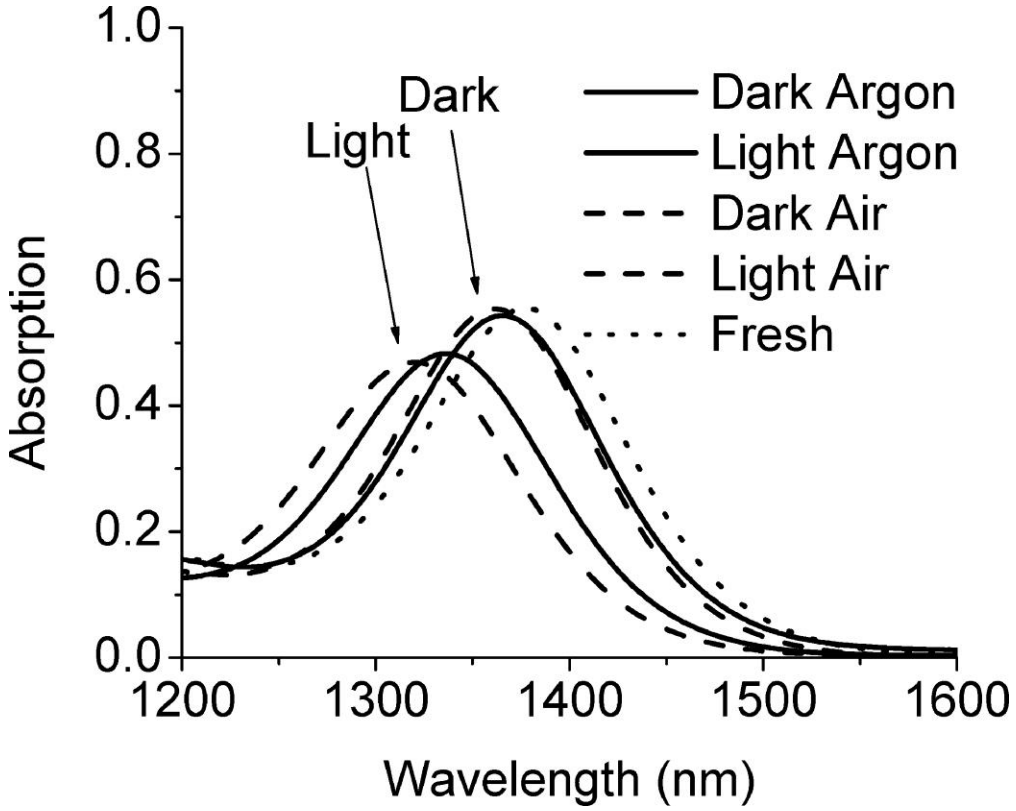

Fig- 1. Absorption spectra of PbSe NCs stored for 42 days under different conditions. The NCs with the largest blue shift compared to the fresh sample were stored in room light; the other two were stored in the dark. The dashed spectra are of NCs stored under ambient conditions; the solid lines are of NCs stored under Ar. Reprinted with Permission from [19]. Copyright 2007, American Chemical Society.

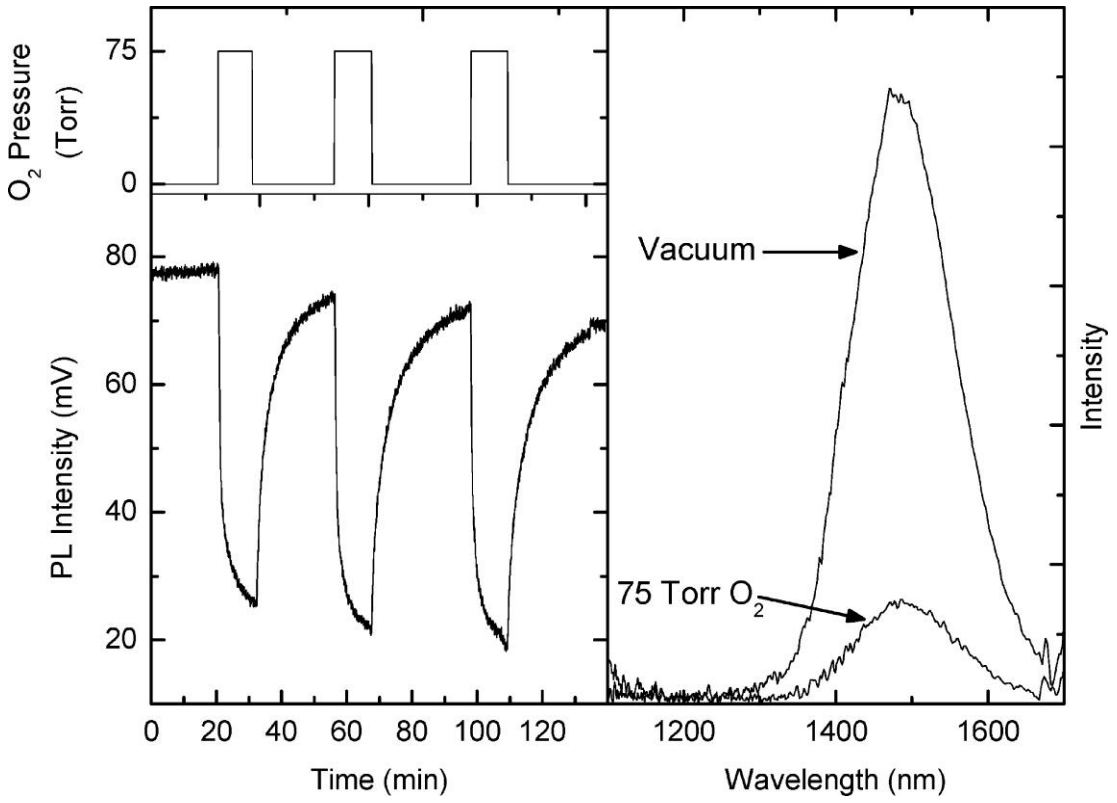

Fig- 2. (Left) PbSe luminescence quenching by repeated 11 min exposures to 75 Torr of O2. (Right) PbSe luminescence spectra under vacuum and O2. Reprinted with Permission from [19]. Copyright 2007, American Chemical Society.

While we looked at the stability of the QDs, the usage of TOP (trioctyl phosphine) in the synthesis seem to be an important parameter in obtaining good quality PbSe and PbS QDs. For instance the usage of TOP in PbSe synthesis yielded very good chemical yield and high quantum yield, however the mechanism behind the effect of TOP on growth and quality of these QDs remain unknown (in part because there was no appreciable amount of TOP in the isolated product). To understand more about the synthesis, the effect of such reducing agents on the synthesis of PbSe QDs was studied in much more detail by Bawendi and coworkers [23] which was followed further by Klimov and co-workers [24]. The synthesis of PbSe QDs involves the use of TOP as one of the coordinating ligands. Bawendi and coworkers investigated the growth

process investigated the growth process of PbSe QDs and proposed two mechanisms [23]. The first mechanism the authors proposed was that selenium was reduced to Se^{2-} and it reacted with Pb^{2+} to form the monomers. This was supported by monitoring the reaction which showed an increase in amount of TOPO and the formation of an anhydride. These two products will be formed only if the selenium is reduced. This was ascertained by the fact that free TOP was produced during the reaction instead of an anhydride and TOPO. In case of the second mechanism, selenium is not reduced, but it is presented as elemental selenium to a reduced Pb^{o} species to form the monomer. The increase in free TOP suggests that Pb^{2+} species is being reduced to Pb^{0} species which then reacts with selenium to form PbSe monomers. This was further confirmed by the fact that when diphenylphosphine was added the reaction yield increased and the amount of free TOP also increased. Both mechanisms occur simultaneously, however the second mechanism becomes a dominant process when a reducing agent like diphenyl phosphine was used. Klimov and co-workers further studied these mechanisms and showed that with the unpurified TOP, the synthesis gives a decent chemical yield of QDs but with a very high photoluminescence quantum yield (85 %) [24]. On the other hand when the TOP was heated to 160 ^{o}C under vacuum to remove all impurities, the reaction gave a very poor chemical yield along with a poor photoluminescence quantum yield (~ 2-5%). From NMR spectra the authors infer that the dialkyl-phosphine impurities present in TOP are responsible for the high quality PbSe QDs obtained. When they repeated the synthesis using diphenyl phosphine followed by Bawendi and coworkers it greatly improved the chemical yield, but the photoluminescence quantum yield was very poor. Instead of a strong reducing agent, when a mild reducing agent 1,2-hexadecanediol along with purified TOP (no impurities) was employed it resulted in a high quantum yield for the QDs with chemical yield better than that of using unpurified TOP for the synthesis.

2.2. Synthesis of PbS QDs

The synthesis of PbS is similar to that PbSe QDs. The first PbS QDs with a size dipersion of 15 to 20% were synthesized through an organometallic route in 2003 by Hines *et al.* [25]. They measured a photoluminescence quantum yield of 20% for these QDs. The TEM for the freshly prepared PbS did not look uniform, however there was size focusing [26] during storage which resulted in uniform size dispersion after about 96 hours. The authors speculate that the as-synthesized QDs are not energetically favored due to which they undergo size focusing to reach either a metastable state or a thermodynamic state. No concrete explanation was provided for the self-focusing process observed after synthesis of the QDs. The QDs obtained through this synthesis exhibit a blue shift with respect to their original emission just after the synthesis with improvements in the luminescence intensity a few days after the synthesis. This presents a problem of controlling the QDs to emit at a certain wavelength. In order to improve the stability of QDs and avoid a large size focussing after the synthesis, our group introduced TOP while making the oleates and the ratio of the Pb:S precursors was increased from 1:1 to 22:1 [27]. This change in the experimental conditions resulted in QDs which did not show any size focussing after the synthesis and was very stable in inert conditions. In various solvents, the QDs showed minimal blue shift which is still attributed to photo-oxidation. The change in the reaction mixtures resulted in a very narrow size distribution of the QDs (20 meV is the FWHM, full width at half maximum, for the emission peak) when compared to the previous syntheses (170 to 200 meV FWHM for the emission peak) [25, 28]. Even though improvements were observed with our group's modified synthesis, these QDs have to be passivated with an outer shell of a material with a large bandgap. Moreover, the quantum yield of the PbS QDs prepared using the TOP had higher quantum yield when compared to the ones made without TOP. The absolute

quantum yield was measured using an integrating sphere on about 10 batches of quantum dots to confirm whether the results obtained from the synthesis could consistently be repeated. Of these ten batches, 2 had very high quantum yields (QYs) in the range of 80 %, 6 were in the range of 40-60%, and 2 had a very low QY. This variability in QY is an indication that the reproducibility of this colloidal synthesis needs improvement. The usage of TOP has helped researchers to optimize the synthesis and make QDs of varying size ranging from 2 to 10 nm with increased monodispersity. Zeger Hens and co-workers have shown that the stability of the PbS QDs could further be improved by performing a ligand exchange process [29]. Generally, ligand exchange process results in the etching of lead-based QDs thereby reducing their stability. The oleyl amine ligands present on the surface were exchanged with oleic acid. After the QDs were modified, the absorption peak did not shift for about 6 weeks under atmospheric conditions. The one thing which the authors could have done is to compare how the quantum dots synthesized with their procedure compare with the QDs with TOP and oleic acid synthesized by our group and other groups. This could have helped in further understanding the advantages of their synthesis when compared to other syntheses in literature.

2.3 Core/shell PbSe/CdSe and PbS/CdS QDs

Even with these modifications, the QDs were not stable under ambient light and in the presence of oxygen. A few groups, including ours, tried to grow a passivating shell over the QDs to improve their stability. In general quantum dots based on cadmium essentially face the same issue of stability, which has been solved by growing a passivating shell like CdS or ZnS [30]. These cadmium-based quantum dots have been passivated with a shell using the classical epitaxial growth. Peng and co-workers came up with a very efficient technique called successive ion layer adsorption and reaction (SILAR) to grow a passivating shell of ZnS over CdSe [31].

Recently, giant core/shells of CdSe/CdS have been grown using the epitaxial growth method [32-33]. These giant core/shells exhibit minimal blinking. Bawendi and co-workers modified the CdSe/CdS core/shell synthesis to form thin CdSe/CdS core/shells which show very minimal blinking properties and have a quantum yield close to unity [34]. The same principle of epitaxial growth was applied to grow a passivating shell for the lead-based QDs (PbSe and PbS). Generally a shell of CdS or CdSe has to be grown to in order to passify the PbSe or PbS QDs. However the shell growth did not occur like what was observed for cadmium based quantum dots [35]. To overcome this obstacle, Hollingsworth and co-workers utilized the cation exchange process to grow a passivating shell [35]. The concept of cation exchange to grow heterostructured materials was first shown by Alivisatos and co-workers [36-37]. In their report, in presence of excess silver ions the CdSe QDs were converted to Ag_2Se QDs of the same size and shape [37]. The amount of silver ions is in slight excess than the total amount of cadmium ions which are to be replaced. The silver ions were taken in excess in order to facilitate the cation exchange process to occur. They could also exchange silver cations in the Ag_2Se NCs with cadmium ions back to the CdSe NCs through the same cation exchange process. For the reverse process the amount of excess cadmium ions required is about 50 to 100 times with respect to the amount of silver ions to be replaced. The cation exchange process was also observed with anisotropic structures. The same principle was applied in case of the PbSe and PbS QDs to obtain heterostructures [35]. The PbSe or PbS QDs were exposed to excess cadmium oleate at a temperature of 100 ^{o}C for a reaction time of 19 hours. This resulted in a process similar to what Alivisatos and co-workers had observed. However, instead of a complete cation exchange between the cadmium and lead ions Hollingsworth and co-workers observed a partial cation exchange which resulted in a core/shell structure [35]. The partial cation exchange occurs because of the use of a slow reacting cadmium precursor which is soluble in a non-coordinating solvent in

addition to its dependence on the temperature of the reaction and the amount of excess cadmium employed. The core/shell structure was given evidence by the fact that the emission of the core/shell PbSe/CdSe QDs were blue shifted when compared with the core PbSe QDs (Figure 3). This suggests that the core size had effectively shrunk and a shell of CdSe had formed. The modified QDs exhibited remarkably improved stability in ambient light and atmosphere when compared to the core QDs. The paper also mentions that the ZnS shell can be grown over the core/shell QDs, however, the synthesis has to be optimized in order to achieve the best possible optical properties and stability (Figure 4). The core/shell PbSe/CdSe or PbS/CdS and core/shell/shell PbSe/CdSe/ZnS or PbS/CdS/ZnS showed remarkable improvement in stability under ambient conditions. The authors observe that the quantum yield did not increase much if the initial quantum yield of the core/shell QDs is quite high. The authors also add that they did not observe complete cation exchange at temperatures they employed for the cation exchange reaction. This is the seminal work on core/shell QDs of lead-based quantum dots which showed improvements in stability of the QDs under atmospheric conditions. However, the fact that whether a proper core/shell structure (proper core/shell refers to the fact whether a uniform shell has been formed around the core) was formed by the cation exchange process remained unanswered. Hollingsworth and coworkers employed elemental analysis and photoluminescence spectra to substantiate their claim for core/shell structure. TEM images provided by them did not actually give any contrast difference due to the fact that very thin shells of CdSe has been formed over the PbSe core. To answer that question our group investigated the cation exchange process in much more detail. Lambert *et al.* have shown excellent contrast between PbSe core and PbSe/CdTe core/shell QDs through HR-TEM [38].

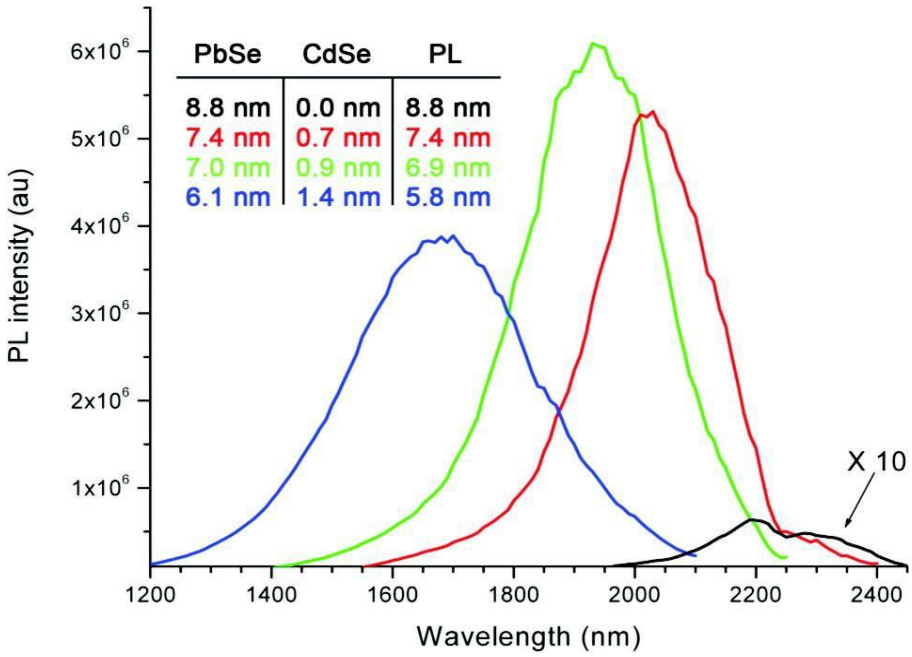

Fig- 3. PL spectra from a series of aliquots during CdSe shell formation, corresponding to 15 min, 2 h, and 24 h of reaction time proceeding from red to blue. Each spectrum is corrected for variation in optical density as well as grating and detector efficiencies to reflect relative QY. Shown in black is the original PbSe core, magnified 10-fold so its shape is discernible. The inset lists the calculated core diameter (column "PbSe") and shell thickness ("CdSe") from elemental analysis. Also included is the approximate effective core size predicted by the PL peak position. Reprinted with Permission from [35]. Copyright 2008, American Chemical Society.

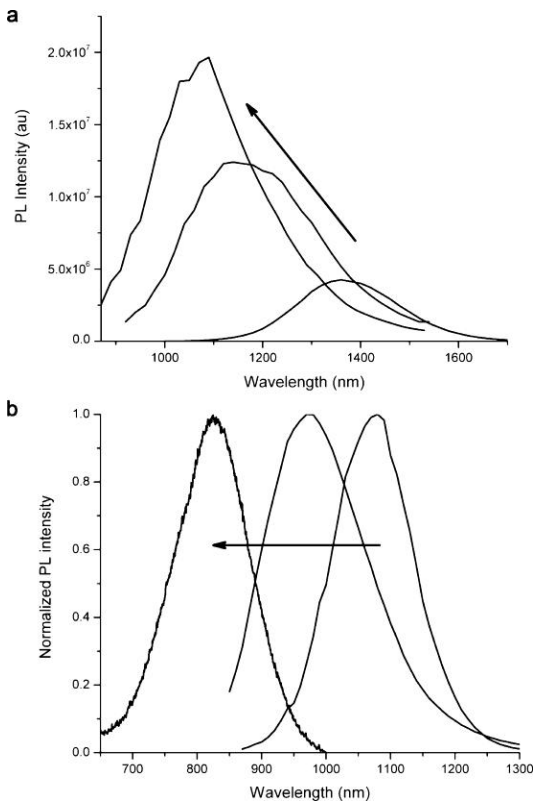

Fig – 4. PL spectra of PbS and PbS/CdS NQDs. Arrows indicate progress of reaction during CdS shell formation: (a) spectra of larger (~ 7 nm) PbS and two aliquots during CdS shell formation, showing relative PL enhancement during the process; (b) normalized spectra of smaller (~ 5nm). PbS and PbS/CdS NQDs with PL as blue as 830 nm. The bluest spectrum was collected on a Ocean Optics USB2000 spectrometer, making direct comparison of peak intensities difficult. PL peaks have been normalized for easier comparison of position and shape. QYs for the bluest PbS/CdS NQDs are typically 20−30%. Reprinted with Permission from [35]. Copyright 2008, American Chemical Society.

Our group followed up this work to provide concrete evidence that a core/shell structure can indeed be formed as suggested by Hollingsworth and co-workers by very carefully controlling and optimizing the reaction conditions. The conditions for the cation exchange were carefully tuned by taking into account of the temperature of the reaction, excess cadmium oleate and the

amount of the lead QDs. Convincing proof for the core/shell lead-based quantum dots was obtained by using High-Angle Annular Dark-Field Imaging (HAADF), Energy-Filtered Transmission Electron Microscopy (EF-TEM), and energy-dependent X-ray Photo-electron Spectroscopy (XPS) [39]. It was also found that depending on the temperature and the amount of the excess cadmium oleate employed for cation exchange, we observed either a partial cation exchange or a complete cation exchange. Hollingsworth and coworkers changed the temperature of the cation exchange reaction but did not change the amount of excess cadmium oleate. Changing both parameters results in complete cation exchange. After complete exchange, the CdSe formed had the same crystal structure as the core PbSe QDs, contrary to the direct synthesis of CdSe QDs. This is consistent with the fact a core/shell structure occurs through the cation exchange process while the anionic lattice remains essentially unperturbed. The HAADF images (Figure 5c) after the cation exchange process shows a discernible contrast difference between the core and the shell. However, the interface between the core and shell is not very clear, which could in principle be from some alloying. However, the contrast in HAADF imaging is not necessarily due to the core-shell respective chemical compositions, because strain may also contribute to the contrast. To obtain extra evidence energy-filtered Scanning Transmission Electron Microscopy (STEM) was performed. The lead mapping (Figure 5a) is observed only in the centre of the particle where as the selenium mapping (Figure 5b) is seen throughout the whole QD. This is fully consistent with the formation of a core/shell structure. There is a lot of beam damage observed while imaging the QDs. Hence, it is imperative that a bright-field image is taken to check the stability of the QDs before and after the EF-TEM. In addition, careful examination of the HR-TEMs in the supporting information suggests that indeed not all cation-exchanged QDs are indeed “proper” core-shell structures; proper in the sense that the shell is of uniform thickness around the core. From energy-dependent XPS measurements it was found

that the Pb/Cd ratio increased with increasing photo-electron kinetic energies implying that the lead is in the center and the Cd is on the surface, as expected for a core-shell structure. Furthermore, in order to understand the structure of the core and core/shell nanoparticle our group performed high-resolution XPS measurements. The high-resolution XPS measurements of PbSe core nanocrystals showed that the chemical speciation of lead on the surface of the nanocrystal is different from the one inside as the surface lead ions are coordinated to either the oleates or the TOP. In case of core/shell PbSe/CdSe nanoparticles the high-resolution XPS spectra show that it can be assumed that a very thin interface of $Pb_{(1-x)}Cd_xSe$ is present between the core PbSe and the shell CdSe. It would be interesting to study these materials with Extended X-ray Absorption Fine Structure (EXAFS) and X-ray Absorption Near Edge Structure (XANES) to obtain more data on the interface between the core and the shell. This would potentially help in developing a mechanism for the cation exchange process. Performing high-resolution XPS and X-ray absorption spectroscopy (XAS) measurements during the reaction might also yield important details on the cation exchange process.

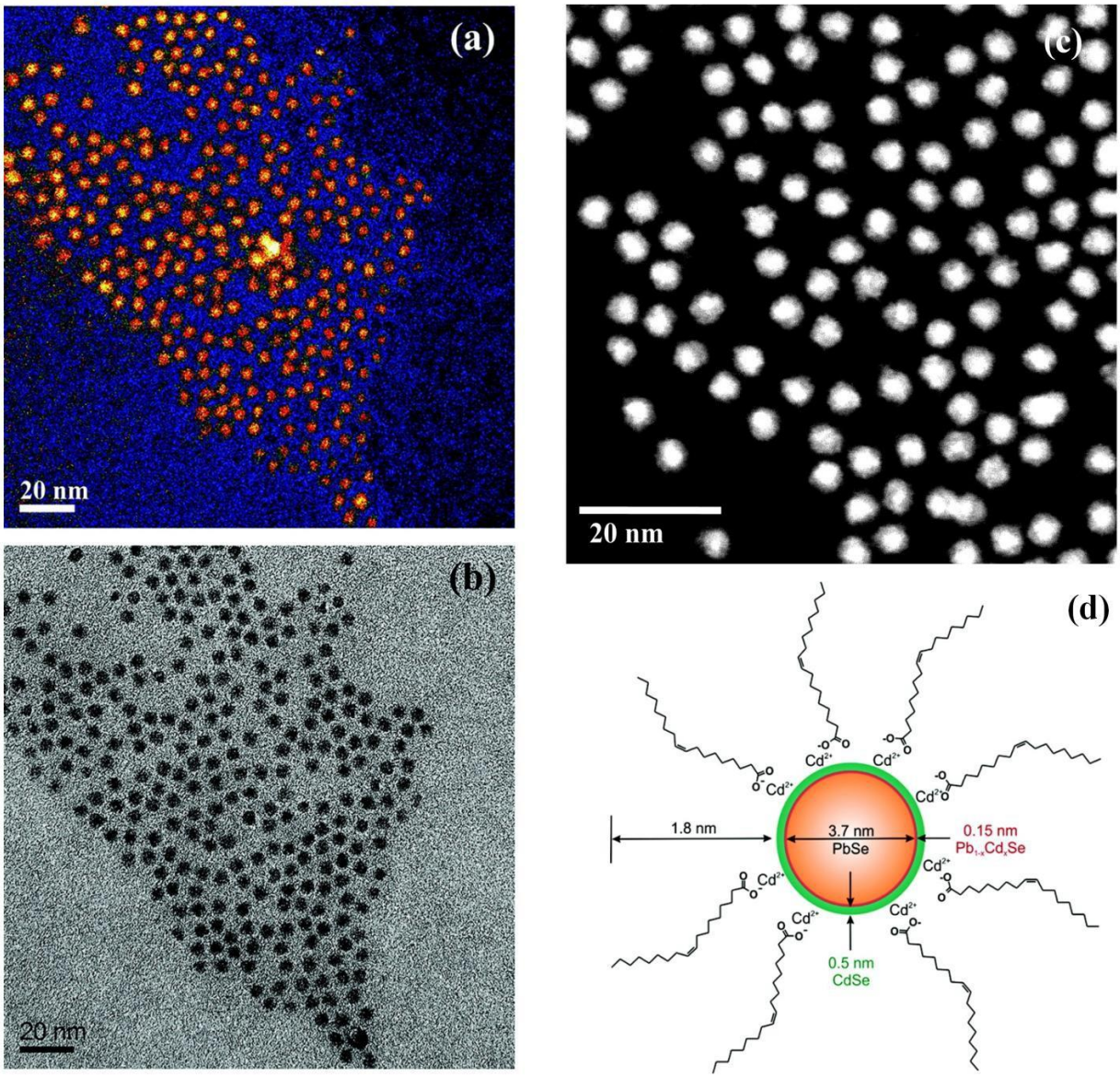

Fig-5. (a) Pb mapping of core/shell PbSe/CdSe QDs (b) Imaging of the same QDs after the EF-TEM (c) HAADF images of PbSe/CdSe QDs (d) Schematic representation of the core/shell PbSe/CdSe QDs. Reprinted with Permission from [39]. Copyright 2012, American Chemical Society.

Hollingsworth and coworkers in their work to obtain core/shell structures of lead-based QDs, also mention that at 110^{o}C temperatures the cation exchange is partial which results in a

core/shell structure [35]. They tested this hypothesis by allowing the reaction to continue for a long time (19 hours). The Cd^{2+} cations which will replace the lead ions on the QDs are taken in large excess to drive the process. The authors performed the reaction at one specific temperature (110 ^{o}C). We speculate that the cation exchange process is driven by mass transfer, surface and crystal defects of the lead-based quantum dots. As these factors do not have the same influence on each quantum dot, they could be a reason for the non-uniform shell of CdSe over PbSe. This can clearly be observed from Figure 5C. Our group performed the cation exchange process at different temperatures starting from room temperature to 130 ^{o}C and found that at high temperatures complete cation exchange could be observed. The amount of cadmium oleate taken was also increased when compared to Hollingsworth's report. By changing the temperature the cation exchange can be controlled to obtain the desired emission wavelength. It thus seems that this cation-exchange process is very sensitive to the reaction conditions. The cation exchange process is very efficient in terms of increasing the resistance towards photostability and photo-oxidation. It also increases the quantum yield of the nanocrystals if the core nanocrystals had a poor quantum yield in the first place. One important observation made by our group is that the cation exchange occurs faster in case of smaller nanocrystals when compared to the larger ones [39]. This could be due to the large surface to volume ratio and the higher surface energy of the smaller nanocrystals when compared with the big ones. It could also potentially be due to a larger surface defect concentration in the smaller QDs. One other important observation made is that the FWHM for the PL from core/shell PbSe/CdSe QDs are larger than the core PbSe QDs (Figure 4b). This is consistent with the cation exchange process being not very uniform on all core PbSe QDs coupled with the fact that faster cation exchange rates were observed for smaller QDs when compared with the larger ones. This results in the larger size distribution of the core

PbSe QDs thereby increasing the FWHM for the PL from the QDs [40]. The mechanism behind the cation exchange process for the growth of core/shell lead-based QDs is not yet understood in this case. It would be very interesting to understand the mechanism behind the formation of a core/shell structure. There are a few questions which could be answered by understanding the process.

1) Why does the cation exchange stop at a certain point during the reaction to form a core/shell structure even if it is carried out for a very long time at high temperatures like 100 ^{o}C.
2) Whether (surface) defects play a significant role in the cation exchange process because smaller QDs undergo a faster cation exchange process than the large QDs. One possible mechanism is a cation hopping through a vacancy in the QD.

Hollingsworth and coworkers also demonstrated that a ZnS shell can be grown over the PbSe/CdSe and PbS/CdS core/shell QDs. Optimizing the ZnS shell growth over the core/shell PbSe/CdSe would further increase the stability of these QDs and enable the surface to be manipulated rather easily. A ZnS shell would make these QDs very similar to CdSe/ZnS QDs for which the surface engineering has been developed and studied in great detail. The presence of ZnS could in theory reduce the toxicity of these quantum dots if they are to be employed for biological applications. The tuning of the emission through cation exchange process helps in obtaining QDs with very high quantum yield which emit around 800 nm. The emission at 800 nm would enable researchers to perform two photon microscopy based imaging using these QDs by exciting them at 1250 nm. Both the excitation and emission wavelength lie in a region where the tissue is very transparent which could aid in imaging deeper inside animals. This will propel the field towards employing these nanocrystals for optical bio-imaging.

3. Surface Modification of Lead-based QDs

Surface modification of the QDs is essential for bio-applications due to the fact that they have to be made biocompatible. There are only a handful of reports which have been able to show surface modification on lead-based QDs. The first report on surface modification was on PbSe QDs which was done by Colvin and coworkers. A small molecule 11-mercaptoundecanoic acid was used to replace the oleates on the surface of the PbSe QDs to disperse them in water [18]. The process resulted in a dispersion of QDs stable in water for a few days but not in physiological buffers. Following this, the same process was utilized to image human colon cells using PbSe and PbS QDs by Wise and coworkers [41]. Few groups have tried to coat the PbSe QDs with silica through the reverse microemulsion process [42-43]. Both reports show uniform coating of the QDs, however, no emission has been reported after the coating (Figure 7). Until now, only Colvin and the Wise groups have been able to show emission from PbSe QDs after the surface modification [18]. In general PbSe QDs are less stable when compared to the PbS QDs which also seems to be major detrimental factor in modifying the surface to disperse them in water. On the other hand, surface modification of PbS QDs either through ligand exchange or silica coating or intercalation process has resulted in the emission being retained after the process. The first report on surface modification of PbS QDs was by Hinds *et al.* who functionalized the mercaptoundecane chain with tetra-ethylene glycol, which was then used for the ligand exchange process to render the PbS QDs dispersible in water [28]. The PbS QDs exhibited colloidal stability in 4-(2-hydroxyethyl)-1-piperazineethanesulfonic acid (HEPES) buffer for about 5 days after which they started to settle down. Small ligands, like the above mentioned ones, in general do not impart the same stability to PbS QDs as observed for other nanocrystals. This could possibly be due to the irreversible replacement of ligands on the surface

of the QDs due to the dynamic nature of the ligands. The interesting factor to note in this process is that after the ligand exchange process, the emission profile of the QDs shifted towards the red (Figure 6). The thiol-lead bond changes the electronic density and confinement of the QD which results in the red shift after surface modification. It could also be due to the growth which could have occurred due to the ligand exchange process. Winnik and coworkers also performed ligand exchange on the PbS QDs with polyacrylic acid to transfer them to water [44]. After the exchange process, the photoluminescence quantum yield dropped and eventually the emission was completely lost after some days. The access of water molecules to the surface of the QDs and the rapid oxidation process which happens due to the presence of dissolved oxygen in water is led to have resulted in a poor quantum yield and loss of emission over time. The only advantage of this process over the ligand exchange with small molecules is that the dispersion was stable over long periods of time even though the emission is lost after a few days. Moreover, there is unfortunately nothing mentioned in the report about their colloidal stability in various buffers.

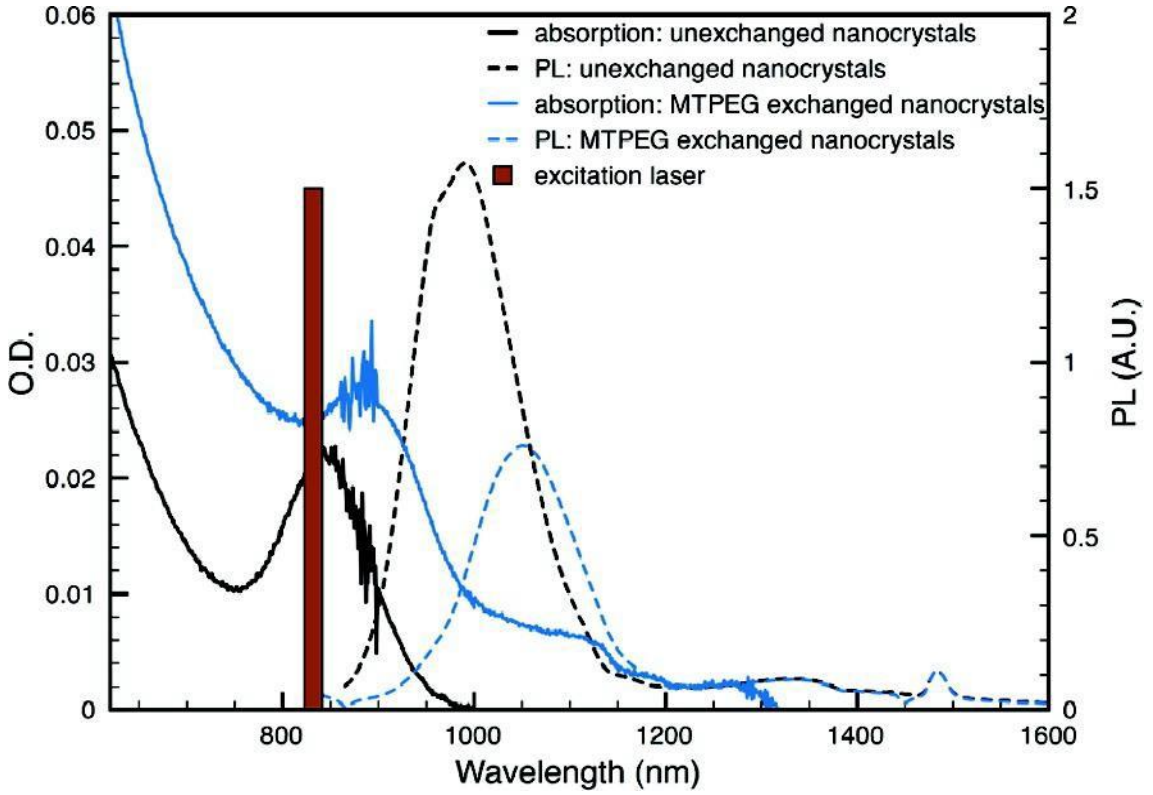

Figure 6. Absorption and luminescence spectra of (~10 mg/mL) PbS quantum dots prior to and following exchange to aqueous solution. Solid lines represent absorption spectra. Dashed lines represent photoluminescence spectra. Dark lines represent original OA capped PbS nanocrystals in toluene. Gray lines represent MTPEG-exchanged capped PbS nanocrystals in 20 mM HEPES buffer. Solid bar represents excitation wavelength used for PL spectra collection. Reprinted with Permission from [28]. Copyright 2008, American Chemical Society.

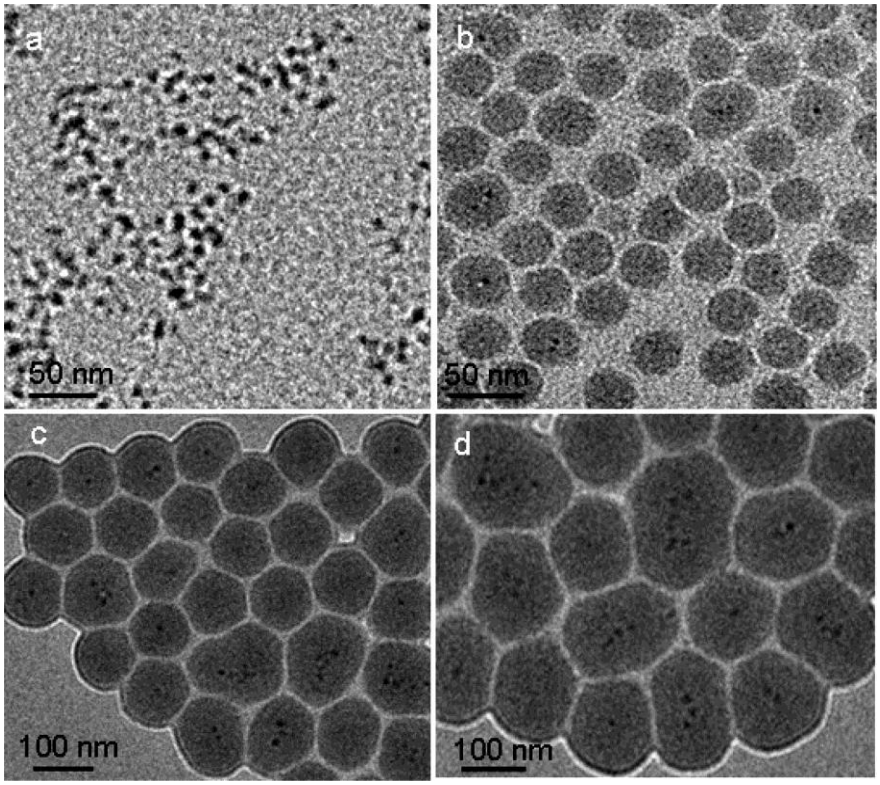

Figure 7. TEM images of SiO_2/PbSe nanoparticles prepared in Igepal reverse microemulsion with (a) 2, (b) 10, (c) 50, and (d) 100 μL of TEOS. The average particle diameter varies from ~40 to 160 nm with an increase in TEOS volume (b−d). Reprinted with Permission from [43] Copyright 2008, American Chemical Society.

Coating of silica on PbSe QDs resulted in the loss of emission, on the other hand, Xu *et al.* have shown emission from PbS QDs after coating them with silica [45]. The important factor is that the emission shifts towards the blue after the silica coating which implies that the QDs have been etched during the process. In addition to the ligand exchange process and silica coating two groups have employed the intercalation process to render the PbS QDs dispersible in water [46-49]. Ma and coworkers have employed poly(maleicanhydride-*alt*-1-octadecene) (PMAO) modified with polyethylene glycol (PEG) to transfer PbS QDs from hydrophobic phase to hydrophilic phase [44]. As the first step, 30 of 110 anhydride rings in the PMAO were reacted

with hydroxyl molecules of PEG in presence of sulphuric acid to make the PMAO dispersible in water. They used the modified polymer to coat the PbS QDs and dispersed them in water. However, the emission did not last for more than 15 minutes. Furthermore, the emission wavelength was shifted towards the blue which suggests etching of the QDs. In order to retain the emission over longer periods of time, the same process was employed to modify the surface of PbS/CdS core/shell QDs. The modified PMAO-PEG polymer coated QDs exhibited photoluminescence with a small blue shift. We suspect that during the modification of the PMAO polymer with PEG molecules there are trace amounts of acid which could be present even after washing. The presence of even trace amounts of sulphuric acid during the modification could as well have resulted in the etching of the QDs and could have acted as a catalyst to open all the anhydride rings in PMAO to form carboxylic acid groups. The presence of a large number of carboxylic acid groups could then have replaced the oleates on the PbS and PbS/CdS QDs. This process becomes effectively a ligand exchange process rather than an intercalation process which generally results in the etching of the QDs. All the above reasons are responsible for the loss of emission in case of PbS QDs and the blue shift observed for the core/shell PbS/CdS QDs. The report mentions that the QDs are stable in buffers, but do not mention the duration of the colloidal stability. In a very recent report in 2012, the authors claim that they have modified 5 nm PbS QDs to disperse in water using amphiphilic polymer micelles which emits around 900 nm before and after surface modification [46]. The fact that there doesn't seem to be a correlation between the quantum confinement effect and the emission wavelength is rather very puzzling to us. The TEM image after modification shows that the one micelle contains several QDs and the size of the micelles are around 190 to 200 nm. This is not ideal for employing them in biological applications. From all the above reports, we conclude that there is a necessity for a methodology which will fulfill the following criteria so that lead-based quantum dots could be employed for

biological applications:

1) Long-term colloidal stability in aqueous media, buffers, and biological media;
2) Colloidal stability in presence of salts and biomolecules;
3) Avoid etching of the QDs and retain the same emission wavelength before and after modification;
4) Provide functionality to the surface so that they can be conjugated to biomolecules.

Our group recently came up with an effective method to disperse PbSe and PbS QDs in water and biological media and maintain their colloidal stability over several months while at the same time retaining their luminescence over the whole period with only small shifts in the luminescence [50]. The PMAO polymer was modified with PEG-amine to open some of the anhydride rings to impart water solubility to the polymer. The octadecene chains in the polymer interdigitate with the oleate chains on the surface of the QDs due to the hydrophobic effect, while the PEG moieties impart dispersibility in aqueous media to the QDs. Following this first modification the rest of the anhydride rings in PMAO present on the polymer were crosslinked using bis(hexamethylenetriamine) which imparted colloidal stability to the QDs over several months (~7 months) in water. When the crosslinked polymer (PMAO-PEG-BHT) coated QDs were dispersed in phosphate, TRIS, and borate buffers the QDs exhibited colloidal stability over 7 months with no signs of settling down. The luminescence was retained with only very minimal change in the emission profile before and after the surface modification in the aforementioned aqueous media (Figure 8 A&B). The stability of these QDs was further tested in a serum-supplemented growth media under two conditions (4 and 37.4 ^{o}C). At 4 ^{o}C the QDs showed stability for about 20 days and at 37.4 ^{o}C the QDs were stable for more than 4 days (Figure 8 C&D). The colloidal stability in different pH values (5 to 14) was also excellent for

7 months (Figure 9). The important aspect of this modification process is that all the surface modified QDs were kept in ambient atmosphere and yet the coated QDs showed resistance towards the oxidation process (Figure 8). The presence of carboxylic acid groups on the surface would enable us to functionalize the QDs with biomolecules like proteins, and antibodies for biological applications. We were able to show similar colloidal stability and luminescence retention for both PbSe and PbS QDs (Figure 10). A ZnS shell over these QDs would further improve their stability and reduce the toxicity of these materials as well.

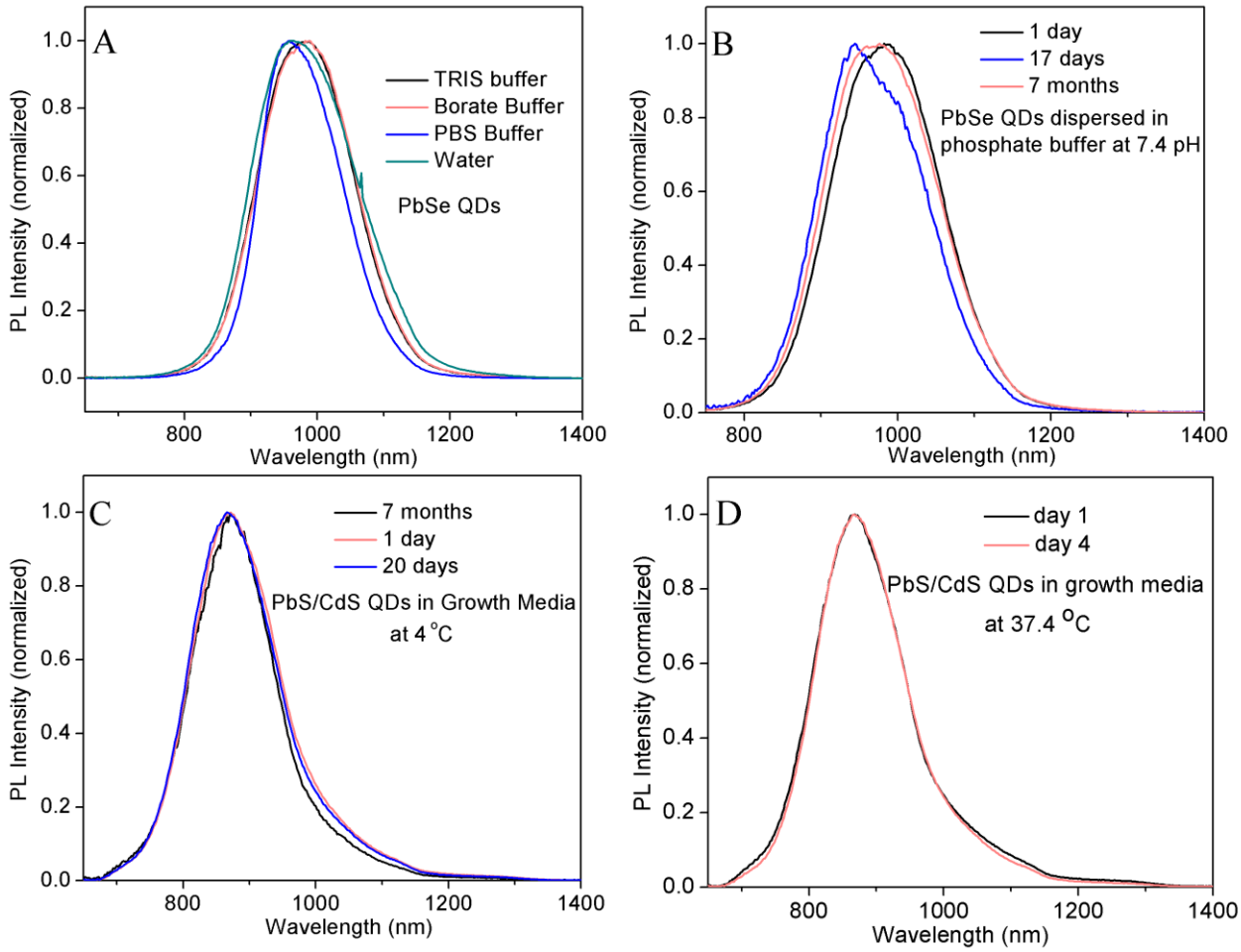

Figure 8. (A) PbSe QDs in various buffers after surface modification with PMAO-PEG-BHMT; (B) PbSe QDs in phosphate buffers at various days; (C&D) PbS/CdS in serum-supplemented growth media at 4, and 37.4 ^{o}C, respectively, after surface modification with PMAO-PEG-

BHMT. Reprinted with Permission from [50] Copyright 2013, American Chemical Society.

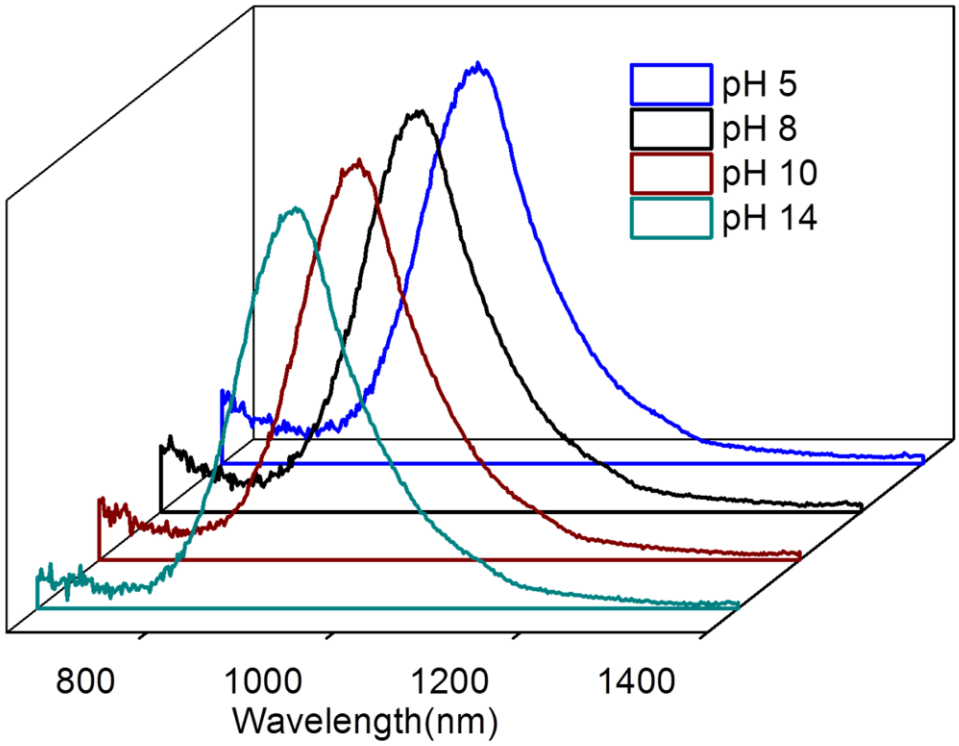

Figure 9 PMAO-PEG-BHMT coated PbS QDs at different pH values. Reprinted with Permission from [50] Copyright 2013, American Chemical Society.

Figure 10. Pictures of dispersion of PbS/CdS and PbSe QDs in TRIS buffer and water, respectively. Reprinted with Permission from [50] Copyright 2013, American Chemical Society.

4. Optical Properties of Lead-based QDs

PbSe QDs exhibit size-dependent optical and electronic properties due the quantum confinement observed in the nanosize regime. Prior reports on the temperature-dependence optical properties of thin films of PbSe QDs have not explained completely the PL shift towards the red and the observed reduction in the values of full width at half maximum (FWHM) for PL at lower temperatures [51-53]. Lifshitz *et al.* employed the phenomenological Varshini equation to fit the PL red shift with very limited success [51]. The phonon scattering model used to explain the FWHM of the PL peaks also resulted in a very moderate success. Additionally, the PbS-polymer blends, PbS QDs as drop-cast films and thin films formed through spin coating exhibit remarkably different temperature-dependent optical properties. Hence its very hard to explain

them using conventional phenomenological equations. In addition to the above reports, Dey *et al.* have investigated the strong band gap dependence on temperature of lead based quantum dots [54]. Furthermore Gao *et al.* investigations reveal that chemically treated PbS QDs exhibit temperature dependent quenching and there is a size dependent and ligand binding effect on the motion of carriers between the bright and dark state [55]. The lifetimes of PbSe QDs at very low temperatures and high magnetic fields were studied by Klimov and coworkers [56]. They found that two degenerative states have similar oscillator strength. The lifetimes of the QDs were around 1 μs at 300 K which is predominantly due to the non-radiative decay while the radiative decay values are around 5 μs. They also observed that under high magnetic fields they observed circular polarized infrared emitted light for the first time. Our group has studied the temperature-dependent properties of thick PbSe films drop casted on a silicon substrate [40, 57]. We found that the temperature-dependent PL measurements could easily be repeated with several different batches of QDs which is very big step towards explaining the results as they have to be reproducible. We found that that the PL spectra at low temperatures shift towards the red which has been attributed to the fact that the smaller QDs transfer their energy to the larger ones through the Förster energy transfer mechanism (Figure 11 a&b). Hence a reduction in the FWHM for the PL spectrum was observed. The same case was observed with core/shell PbSe/CdSe quantum dots (Figure 11d). An interesting fact observed was the onset of a non- radiative decay process for the core and core/shell at different temperatures (Figure 11c). Our group found that the activation energy for the non-radiative decay for the core/shell PbSe/CdSe QDs (Figure 12 a&b) is four times as high as the core PbSe QDs. In case of PbSe QDs the activation energy for the non-radiative decay is around 60 K whereas it is around 240 K for the core/shell PbSe/CdSe QDs. The increase in the activation energy is due to the excellent passivation by CdSe which reduces the number of dangling bonds and the surface defects present on the PbSe QDs,

which are potential sites for these non-radiative process (i.e. quenching processes). On the other hand, with the core PbSe QDs there are a large number of dangling bonds coupled with surface effects and the progressive oxidation of the surface. This results in much lower activation energy for the onset of the non-radiative decay processes. The next logical step would be to improve the onset of non-radiative decay till room temperature. The results observed by our group were on a thin shell of CdSe over the core PbSe QDs. Hence a shell of ZnS would in principle further improve the optical properties and the overall stability of the QDs. This could possibly result in advancing the onset of the non-radiative decay above room temperature.

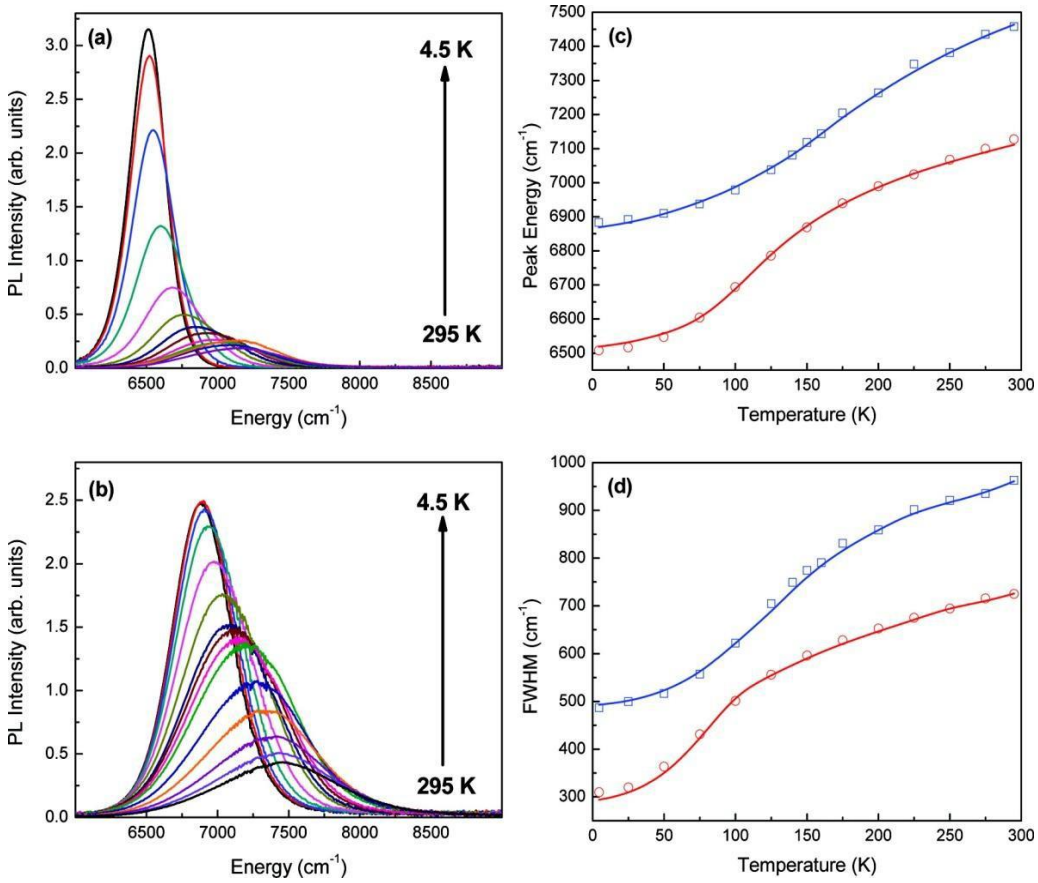

Figure 11. Temperature-dependent PL data for (a) PbSe core and (b) PbSe/CdSe core/shell QDs. (c) Peak energy position (circles: core; squares: core/shell) versus temperature with fit (solid). (d)

The FWHM (circles: core; squares: core/shell) versus temperature with fit (solid). Reprinted with Permission from [40]. Copyright 2011, American Chemical Society.

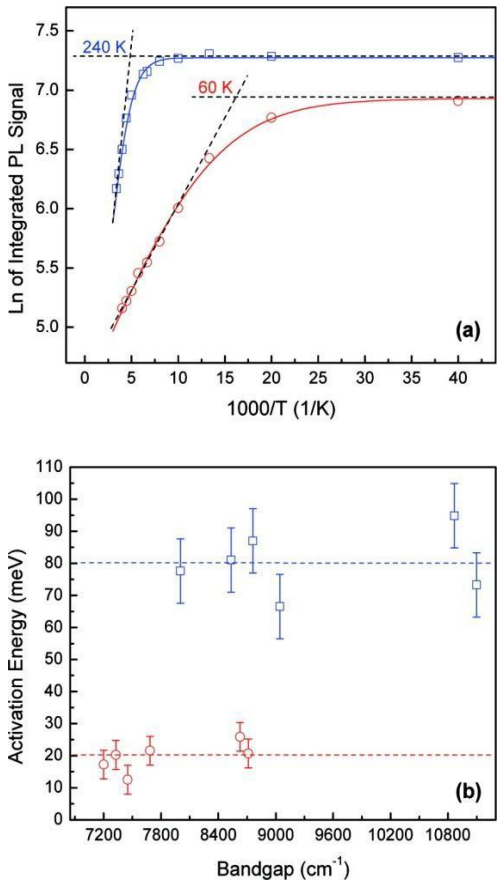

Figure 12. (a) Arrhenius plots for PbSe core (circles) and PbSe/CdSe core/shell (squares) QDs with fits (solid). (b) Measured activation energy for a series of batches of core (circles) and core/shell (squares) QDs. Reprinted with Permission from [40]. Copyright 2011, American Chemical Society.

In addition to our group, Chappell *et al.* have reported that there are two emission states in the PbSe QDs when they were measured as thin films after exposing them to air for 2 min to a maximum of 63 days [58]. The oxidation process occurring due to the exposure to air starts from 2 min and then saturates after several days. When temperature dependent measurements were done there is a flow of population between the two emissive states at lower temperatures. However at higher temperatures this flow is interrupted due to nonradiative trap states which correspond to the

effect of air exposure to the film. The authors finally say that the origin of these two emissive centers needs to be resolved.

5. Other NIR QDs

Cadmium- and lead-free quantum dots are gaining a lot of attention due to their (expected) lower toxicity which makes them benign to the environment. In that class, Ag_2S and Ag_2Se, InP, InAs, InP, CuInSe, CuInS are the major ones [6, 59]. The last two QDs based on copper and indium are the I-III-VI ternary quantum dots. The InAs QDs have exhibited appreciably high quantum yields (35 to 50 %) when a passivating shell of CdSe or ZnCdS or ZnSe or ZnS was grown [60-63]. Bawendi and coworkers again showed that the InAs QDs with a passivating shell could be potential NIR imaging agents for cells and animals [61]. They were able to tune the emission of the QDs between 800 to 1400 nm, after which the quantum confinement is lost for these QDs. $CuInSe_2$ are alternatives to the cadmium and lead-based quantum dots which are toxic due to the presence of heavy metals. The CuInSe and CuInS are I-III-IV ternary semiconductor quantum dots. The synthesis for these QDs is not yet very well developed and the quantum yield is not as high as the lead-based QDs and InAs QDs. Bawendi and coworkers have shown that the band gap of CuInSe can be tuned between 1.3 to 1.74 eV [60]. The disadvantage of not being able to tune the emission over a broad wavelength in the NIR region coupled with their poor quantum yield may limit their applicability. All the above mentioned QDs are very useful for bioimaging as they will be far less toxic than the cadmium and lead-based QDs. Only InAs QDs with a passivation shell has shown decent quantum yield even after dispersing them in water (Figure 13). Pang and coworkers have shown that Ag_2Se QDs can be prepared which can emit between 800 to 1300 nm with a quantum yield of 9 to 10% in organic solvents and about 3 % in water [64-65]. Dai and coworkers have synthesized Ag_2S nanocrystals which emitted around 1200 nm [66-67]. The interesting fact to note was the emission did not shift with the increase in size

which does not correlate with the explanation for a quantum dot. Could this be a defect-related emission? The silver sulphide nanocrystals synthesized by Dai and coworkers had a quantum yield of 30 % [67]. All the synthetic methodologies for the non-cadmium based QDs have to be improved in order to be applicable in biology. The monodispersity and the quantum yield of the aforementioned nanocrystals have to be improved in order to make them viable for applications in the NIR region. Hence for applications in telecommunications, solar cells, and quantum cryptography lead-based QDs seem to be a very viable choice.

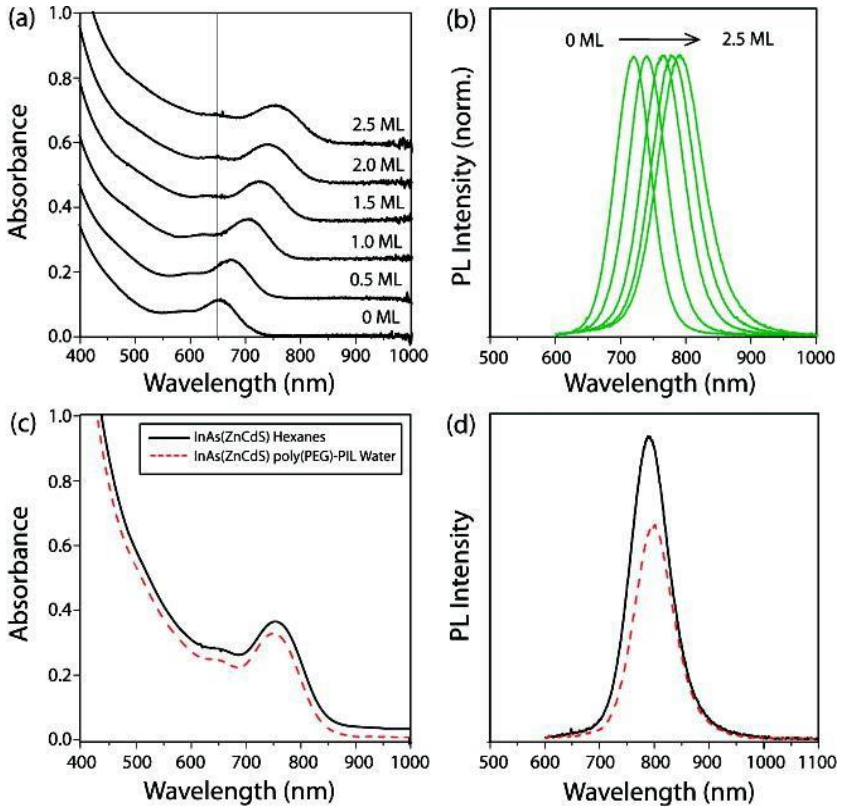

Figure 13. (a−b) Absorbance and PL of InAs($Zn_{0.7}Cd_{0.3}S$) during shell growth from 0−2.5 monolayers (MLs). (c−d) Absorbance and PL (λ_{max} = 795 nm, FWHM = 82 nm) of InAs(Zn0.7Cd0.3S) in hexanes (black) and after ligand exchange with poly(PEG12)-PIL (red) in PBS at pH 7.4. Reprinted with Permission from [61]. Copyright 2010, American Chemical Society.

6. Conclusions

The last decade saw the emergence of NIR emitting lead-based quantum dots which have great potential applicability in the field of solar cells, bioimaging, telecommunications, and quantum computing. The synthetic procedures developed for the core PbS and PbSe QDs have resulted in a high PL quantum yield values of around 70 to 90 % (but these may be the best results on one batch, because the reproducibility of these colloidal syntheses is not easy to realise). Moreover, the seminal work by Hollingsworth and coworkers to synthesize core/shell lead-based QDs dramatically improved their stability in ambient conditions [9]. There are, however, several aspects that still need to be studied in more detail. A uniform ZnS shell over the core/shell lead-based QDs would make these QDs very viable and stable and environmentally benign as well. Combined with a ZnS shell, a general methodology to disperse these nanocrystals in water and buffers would pave the way for employing these nanocrystals as biomarkers for studies in small animals. The next challenge in the improvement of the PL properties would be to increase the onset of non-radiative decay processes to above room temperature, which will open up new possibilities and avenues for these QDs.

Acknowledgements

The authors acknowledge The Canada Foundation for Innovation (CFI), The British Columbia Knowledge Development Fund (BCKDF), and Natural Science and Engineering Council of Canada (NSERC) for their financial support.

References

[1] G.D. Scholes, G. Rumbles, *Nat. Mater.* (2006) *5* 683–696.

[2] F.W. Wise, *Acc. Chem. Res.* (2000) *33* 773–780.

[3] V.I. Klimov, Nanocrystal Quantum Dots, Taylor and Francis Group, LLC, (Boca Raton), (2010).

[4] C.B. Murray, C.R. Kagan, M.G. Bawendi, *Annu. Rev. Mater. Sci.* (2000) *30* 545-610.

[5] C.B. Murray, S.H. Sun, W. Gaschler, H. Doyle, T.A. Betley, C.R. Kagan, *IBM J. Res. Dev.* (2001) *45* 47–56.

[6] E. Cassette, M. Helle, L. Bezdetnaya, F. Marchal, B. Dubertret, T. Pons, *Adv. Drug Delivery Rev.* (2012) http://dx.doi.org/10.1016/j.addr.2012.1008.1016.

[7] S. Keuleyan, E. Lhuillier, P. Guyot-Sionnest, *J. Am. Chem. Soc.* (2011) *133* 16422-16424.

[8] D.E. Gomez, M. Califano, P. Mulvaney, *Phys. Chem. Chem. Phys.* (2006) *8* 4989-5011.

[9] A.L. Rogach, A. Eychmüller, S.G. Hickey, S.V. Kershaw, *Small* (2007) *3* 536–557.

[10] J.M. Pietryga, R.D. Schaller, D. Werder, M.H. Stewart, V.I. Klimov, J.A. Hollingsworth, *J. Am. Chem. Soc.* (2004) *126* 11752-11753.

[11] A. Sashchiuk, L. Langof, R. Chaim, E. Lifshitz, *J. Cryst. Growth* (2002) *240* 431-438.

[12] R.B. Vasiliev, S.G. Dorofeev, D.N. Dirin, D.A. Belov, T.A. Kuznetsov, *Mendeleev Commun.* (2004) 169-171.

[13] C.E. Finlayson, A. Amezcua, P.J.A. Sazio, P.S. Walker, M.C. Grossel, R.J. Curry, D.C. Smith, J.J. Baumberg, *J. Mod. Opt.* (2005) *52* 955-964.

[14] M. Brumer, A. Kigel, L. Amirav, A. Sashchiuk, O. Solomesch, N. Tessler, E. Lifshitz, *Adv. Funct. Mater.* (2005) *15* 1111–1116.

[15] M. Brumer, M. Sirota, A. Kigel, A. Sashchiuk, E. Galun, Z. Burshtein, E. Lifshitz, *Appl. Opt.* (2006) *45* 7488-7497.

[16] B.L. Wehrenberg, C. Wang, P. Guyot-Sionnest, *J. Phys. Chem. B* (2002) *106* 10634–10640.

[17] H. Du, C. Chen, R. Krishnan, T.D. Krauss, J.M. Harbold, F.W. Wise, M.G. Thomas, J. Silcox, *Nano Lett.* (2002) *2* 1321–1324.

[18] W.W. Yu, J.C. Falkner, B.S. Shih, V.L. Colvin, *Chem. Mater.* (2004) *16* 3318-3322.

[19] J.W. Stouwdam, J. Shan, F.C.J.M. van Veggel, A.G. Pattantyus-Abraham, J.F. Young, M. Raudsepp, *J. Phys. Chem. C* (2007) *111* 1086–1092.

[20] I. Moreels, B. Fritzinger, J.C. Martins, Z. Hens, *J. Am. Chem. Soc.* (2008) *130* 15081–15086.

[21] M. Sykora, A.Y. Koposov, J.A. McGuire, R.K. Schulze, O. Tretiak, J.M. Pietryga, V.I. Klimov, *ACS Nano* (2010) *4* 2021–2034.

[22] S. Kim, B. Fisher, H.J. Eisler, M. Bawendi, *J. Am. Chem. Soc.* (2003) *125* 11466-11467.

[23] J.S. Steckel, B.K.H. Yen, D.C. Oertel, M.G. Bawendi, *J. Am. Chem. Soc.* (2006) *128* 13032-13033.

[24] J. Joo, J.M. Pietryga, J.A. McGuire, S.H. Jeon, D.J. Williams, H.L. Wang, V.I. Klimov, *J. Am. Chem. Soc.* (2009) *131* 10620-10628.

[25] M.A. Hines, G.D. Scholes, *Adv. Mater.* (2003) *15* 1844–1849.

[26] X.G. Peng, J. Wickham, A.P. Alivisatos, *J. Am. Chem. Soc.* (1998) *120* 5343-5344.

[27] K.A. Abel, J.N. Shan, J.C. Boyer, F. Harris, F.C.J.M. van Veggel, *Chem. Mater.* (2008) *20* 3794–3796.

[28] S. Hinds, S. Myrskog, L. Levina, G. Koleilat, J. Yang, S.O. Kelley, E.H. Sargent, *J. Am. Chem. Soc.* (2007) *129* 7218-7219.

[29] I. Moreels, Y. Justo, B. De Geyter, K. Haustraete, J.C. Martins, Z. Hens, *ACS Nano* (2011) *5* 2004-2012.

[30] B.O. Dabbousi, J. Rodriguez-Viejo, F.V. Mikulec, J.R. Heine, H. Mattoussi, R. Ober, K.F. Jensen, M.G. Bawendi, *J. Phys. Chem. B* (1997) *101* 9463–9475.

[31] J.J. Li, Y.A. Wang, W.Z. Guo, J.C. Keay, T.D. Mishima, M.B. Johnson, X.G. Peng, *J. Am. Chem. Soc.* (2003) *125* 12567-12575.

[32] Y. Chen, J. Vela, H. Htoon, J.L. Casson, D.J. Werder, D.A. Bussian, V.I. Klimov, J.A. Hollingsworth, *J. Am. Chem. Soc.* (2008) *130* 5026-5027.

[33] B. Mahler, P. Spinicelli, S. Buil, X. Quelin, J.P. Hermier, B. Dubertret, *Nat. Mater.* (2008) *7* 659-664.

[34] O. Chen, J. Zhao, V.P. Chauhan, J. Cui, C. Wong, D.K. Harris, H. Wei, H. Han, D. Fukumura, R.K. Jain, B. M.G., *Nat. Mater.* (2013) *12* 445-451.

[35] J.M. Pietryga, D.J. Werder, D.J. Williams, J.L. Casson, R.D. Schaller, V.I. Klimov, J.A. Hollingsworth, *J. Am. Chem. Soc.* (2008) *130* 4879-4885.

[36] R.D. Robinson, B. Sadtler, D.O. Demchenko, C.K. Erdonmez, L.W. Wang, A.P. Alivisatos, *Science* (2007) *317* 355-358.

[37] D.H. Son, S.M. Hughes, Y. Yin, A.P. Alivisatos, *Science* (2004) *306* 1009-1012.

[38] K. Lambert, B. De Geyter, I. Moreels, Z. Hens, *Chem. Mater.* (2009) *21* 778–780.

[39] K.A. Abel, P.A. FitzGerald, T.Y. Wang, T.Z. Regier, M. Raudsepp, S.P. Ringer, G.G. Warr, F.C.J.M. van Veggel, *J. Phys. Chem. C* (2012) *116* 3968-3978.

[40] K.A. Abel, H. Qiao, J.F. Young, F.C.J.M. van Veggel, *J. Phys. Chem. Lett.* (2010) *1* 2334-2338.

[41] B.R. Hyun, H.Y. Chen, D.A. Rey, F.W. Wise, C.A. Batt, *J. Phys. Chem. B* (2007) *111* 5726-5730.

[42] M. Darbandi, W.G. Lu, J.Y. Fang, T. Nann, *Langmuir* (2006) *22* 4371-4375.

[43] T.T. Tan, S.T. Selvan, L. Zhao, S.J. Gao, J.Y. Ying, *Chem. Mater.* (2007) *19* 3112-3117.

[44] W. Lin, K. Fritz, G. Guerin, G.R. Bardajee, S. Hinds, V. Sukhovatkin, E.H. Sargent, G.D. Scholes, M.A. Winnik, *Langmuir* (2008) *24* 8215-8219.

[45] D. Wang, J. Qian, F. Cai, S. He, S. Han, Y. Mu, *Nanotechnology* (2012) *23* 245701.

[46] J. Cao, H.Y. Zhu, D.W. Deng, B. Xue, L.P. Tang, D. Mahounga, Z.Y. Qian, Y.Q. Gu, *J Biomed Mater Res A* (2012) *100A* 958-968.

[47] H.G. Zhao, M. Chaker, D.L. Ma, *Phys. Chem. Chem. Phys.* (2010) *12* 14754-14761.

[48] H.G. Zhao, D.F. Wang, M. Chaker, D.L. Ma, *J. Phys. Chem. C* (2011) *115* 1620-1626.

[49] H.G. Zhao, D.F. Wang, T. Zhang, M. Chaker, D.L. Ma, *Chem. Commun.* (2010) *46* 5301-5303.

[50] J. Pichaandi, K.A. Abel, N.J.J. Johnson, F.C.J.M. van Veggel, *Chem. Mater.* (2013) *25* 2035-2044.

[51] A. Kigel, M. Brumer, G.I. Maikov, A. Sashchiuk, E. Lifshitz, *Small* (2009) *5* 1675–1681.

[52] W. Lu, I. Kamiya, M. Ichida, H. Ando, *Appl. Phys. Lett.* (2009) *95* 083102.

[53] V. Rinnerbauer, H.J. Egelhaaf, K. Hingerl, P. Zimmer, S. Werner, T. Warming, A. Hoffmann, M. Kovalenko, W. Heiss, G. Hesser, F. Schaffler, *Phys. Rev. B* (2008) *77* 085322.

[54] P. Dey, J. Paul, J. Bylsma, D. Karaiskaj, J.M. Luther, M.C. Beard, A.H. Romero, *Solid State Commun.* (2013) *165* 49-54.

[55] J.B. Gao, J.C. Johnson, *ACS Nano* (2012) *6* 3292-3303.

[56] R.D. Schaller, S.A. Crooker, D.A. Bussian, J.M. Pietryga, J. Joo, V.I. Klimov, *Phys. Rev. Lett.* (2010) *105*.

[57] H. Qiao, K.A. Abel, F.C.J.M. van Veggel, J.F. Young, *Phys. Rev. B* (2010) *82* 165435.

[58] H.E. Chappell, B.K. Hughes, M.C. Beard, A.J. Nozik, J.C. Johnson, *J. Phys. Chem. Lett.* (2011) *2* 889-893.

[59] Q.A. Ma, X.G. Su, *Analyst* (2010) *135* 1867-1877.

[60] P.M. Allen, M.G. Bawendi, *J. Am. Chem. Soc.* (2008) *130* 9240-9241.

[61] P.M. Allen, W.H. Liu, V.P. Chauhan, J. Lee, A.Y. Ting, D. Fukumura, R.K. Jain, M.G. Bawendi, *J. Am. Chem. Soc.* (2010) *132* 470-471.

[62] H.S. Choi, B.I. Ipe, P. Misra, J.H. Lee, M.G. Bawendi, J.V. Frangioni, *Nano Lett.* (2009) *9* 2354-2359.

[63] S.W. Kim, J.P. Zimmer, S. Ohnishi, J.B. Tracy, J.V. Frangioni, M.G. Bawendi, *J. Am. Chem. Soc.* (2005) *127* 10526-10532.

[64] C.N. Zhu, P. Jiang, Z.L. Zhang, D.L. Zhu, Z.Q. Tian, D.W. Pang, *ACS Appl. Mater. Interfaces* (2013) *5* 1186-1189.

[65] Y.P. Gu, R. Cui, Z.L. Zhang, Z.X. Xie, D.W. Pang, *J. Am. Chem. Soc.* (2012) *134* 79-82.

[66] G.S. Hong, J.T. Robinson, Y.J. Zhang, S. Diao, A.L. Antaris, Q.B. Wang, H.J. Dai, *Angew. Chem. Int. Ed.* (2012) *51* 9818-9821.

[67] Y. Zhang, G.S. Hong, Y.J. Zhang, G.C. Chen, F. Li, H.J. Dai, Q.B. Wang, *ACS Nano* (2012) *6* 3695-3702.